



DancingAnt: Body-empowered Wireless Sensing Utilizing Pervasive Radiations from Powerline

Minhao Cui*, Binbin Xie*, Qing Wang*, Jie Xiong*[◇]

*University of Massachusetts Amherst *Delft University of Technology °Microsoft Research Asia
 *{minhaocui, binbinxie, jxiong}@cs.umass.edu *qing.wang@tudelft.nl

ABSTRACT

In recent years, wireless sensing has attracted lots of research attention with a large range of applications enabled. However, several critical issues still hinder wireless sensing from being adopted in daily use: (a) requiring dedicated devices and (or) dedicated signals; (b) limited sensing coverage; and (c) affecting the original function of the wireless technology (e.g., communication). In this work, we propose a new sensing modality, i.e., leveraging the pervasive powerline leakage for sensing. The key observation is that human body can capture such leaked signals, and the received signals vary with body gestures. We design a cheap ring antenna to collect the powerline leaked signals at human body and establish a body-empowered model to sense body motions. We prototype the proposed system with designs spanning both hardware and software. Comprehensive experiments show that the proposed sensing modality can realize a large range of applications in a different way from existing sensing methods. We showcase the powerful capability of this sensing modality using three typical sensing applications: body gesture recognition, sleep posture sensing, and fall detection.

CCS CONCEPTS

- Human-centered computing → Ubiquitous and mobile computing systems and tools.

KEYWORDS

Wireless sensing, body-augmented, powerline RF leakage

Permission to make digital or hard copies of all or part of this work for personal or classroom use is granted without fee provided that copies are not made or distributed for profit or commercial advantage and that copies bear this notice and the full citation on the first page. Copyrights for components of this work owned by others than the author(s) must be honored. Abstracting with credit is permitted. To copy otherwise, or republish, to post on servers or to redistribute to lists, requires prior specific permission and/or a fee. Request permissions from permissions@acm.org. *ACM MobiCom '23, October 2–6, 2023, Madrid, Spain*

© 2023 Copyright held by the owner/author(s). Publication rights licensed to ACM.

ACM ISBN 978-1-4503-9990-6/23/10...\$15.00

<https://doi.org/10.1145/3570361.3613272>

ACM Reference Format:

Minhao Cui, Binbin Xie, Qing Wang, Jie Xiong. 2023. DancingAnt: Body-empowered Wireless Sensing Utilizing Pervasive Radiations from Powerline. In *The 29th Annual International Conference on Mobile Computing and Networking (ACM MobiCom '23), October 2–6, 2023, Madrid, Spain*. ACM, New York, NY, USA, 15 pages. <https://doi.org/10.1145/3570361.3613272>

1 INTRODUCTION

Wireless technologies have become an indispensable part of our every life. While we are using 4G and 5G services, research effort is being devoted to the design of future 6G networks [8]. Besides wireless communication, in the last few years, wireless signals are further utilized for sensing purposes [30]. The basic principle of wireless sensing is that wireless signals vary with human movements and by analyzing the induced signal variation, human movement information can be obtained. A wide range of applications have been realized with wireless sensing such as contact-free gesture recognition [20, 39, 45] and vital sign monitoring [37, 61].

To meet varying requirements of applications, researchers devoted effort to exploiting various kinds of wireless signals for sensing such as sound [26, 64], radio frequency (RF) signal [45, 51, 55] and light signal [13, 32]. However, existing wireless sensing modalities still face one or more of the following practical issues which hinder them from being deployed in real life: (a) requiring dedicated devices and (or) dedicated signals; (b) limited sensing coverage; and (c) affecting the original function of the wireless technology (e.g., communication). Take popular Wi-Fi sensing as an example [30]. It still requires using dedicated Wi-Fi cards such as Intel 5300 and dedicated packets need to be transmitted. The high packet rate (200 Hz) required for sensing greatly affects Wi-Fi communication. Besides, even though the range of Wi-Fi sensing has been progressively increased [51, 61], the sensing coverage still suffers from blockages such as walls.

We thus ask this question: is there a new sensing modality that can utilize truly ambient signals for sensing without interfering with existing communication? In this paper, we

propose to utilize the ambient RF signals leaked from powerlines¹ for sensing. This RF leakage is caused by alternating current in powerlines based on the well-known Maxwell Equations [52]. The leaked RF signals are conventionally considered “bad”. However, we find that such “bad” leaked signal has the potential to be utilized for sensing without incurring any of the issues discussed above. Powerline sensing does not require any dedicated devices as powerlines are already pervasively deployed in buildings. Owing to the low frequency, it can fully cover an area of interest and does not interfere any existing communication bands. The leakage is also stable and independent of home appliance usage.

Although promising, the ultra-low frequency of the leaked signals, i.e., 50/60 Hz fails conventional wireless sensing schemes. The basic principle of wireless sensing is that target movement influences the propagation of wireless signal, causing the signal amplitude or phase to vary. By analyzing the signal amplitude/phase variation, target information can be obtained. However, this principle does not hold for the leaked RF signal from powerlines because the frequency of the leakage is orders of magnitude lower than conventional RF signals used for communication such as Wi-Fi (5 GHz) and LoRa (915 MHz). The signal variation induced by target movement is too small to be utilized for sensing. For example, a chest displacement of 0.5 cm causes the phase of the Wi-Fi signal to vary by 60 degrees but only causes the phase of the leaked 60 Hz signal to vary by 3.6×10^{-6} degrees.

To utilize the leaked low-frequency RF signal for sensing, we consider human body not only as the target but also as part of the receiver. The rationale why human body can be part of receiver is that human body is composed of cells, fluids, bones, tissues and fat, and therefore, it exhibits bio-electric characteristics [53]. When human body is part of the receiver, more precisely, part of the receiving antenna, the body change (e.g., body movement) can cause considerable signal variation which can be utilized for sensing purposes as illustrated in Figure 1. To conclude, human movement influences the propagation medium of wireless signal for sensing in conventional wireless sensing while in this work, *human body becomes part of the antenna and human movement influences the receiving antenna for sensing*.

To capture extremely low-frequency 60 Hz signal, we design a ring antenna which is cheap and convenient for human target to wear. We study the effect of ring size, thickness and material type. When the ring is worn by the target, human body touches the ring and becomes part of the receiving antenna. The strength of the signal captured is much higher when a ring antenna is worn (touching the body) by the target. Another interesting observation is that the collected

¹The powerline in this paper refers to both the powerline in the walls and the power supply of electronic appliances connected to the powerline.

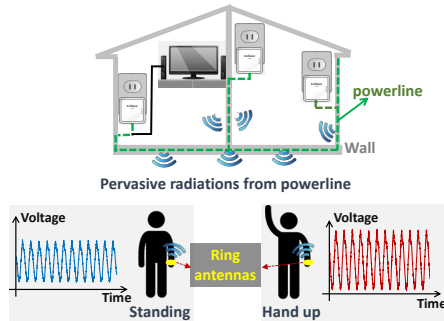


Figure 1: The body collected powerline leakage changes because of the body movement.

signals are roughly the same when the ring is worn at different body positions (e.g., at a finger or at a toe).

After turning human body as part of the sensing receiver, the next challenge is to model the relationship between the received signal and body movement. Existing sensing models [37] consider human body as a reflection object and analyze the signals reflected from human body to infer body movement. In contrast, in our system, the human body acts as part of the receiving antenna instead of the reflection object. We thus need a new sensing model to infer body's movement. We first theoretically analyze the influence of body movement on the received signal. Since the body is now part of the antenna, we would like to study the effect of body movement on the characteristic of the antenna such as shape, impedance and physical location which all affect the strength of the received signal. We observe that, for a same person, stretching out the body captures more energy compared to curling up. Also, standing posture collects more energy than lying down. Besides, a closer distance between body and signal source leads to a larger energy.

The unique advantage of the proposed ring-body antenna is that not only the movement of the finger wearing the ring but the whole body's movement can be detected. This is because the whole body is now part of the antenna. When any part of the body is moving, it changes the antenna's characteristics and accordingly the captured signal varies. However, one challenge still remains, i.e., how to infer which part of the body moves. For example, hand movement and head movement can both induce signal variations. Ideally, we expect the movement of different body parts would induce different signal variations. In practice, we find that the signal variations caused by different body parts can be similar. What makes it worse is that for super-low frequency (50/60 Hz) signal, the phase change which was widely used for finer-grained sensing is too small to be utilized.

To utilize the amplitude information for fine-grained sensing, we leverage another unique feature of powerline's leaked signals, i.e., the leaked signal is stable and continuous compared with RF communication signals. Take Wi-Fi as an

example. Wi-Fi signals are intermittent and vary a lot during communication [7]. In contrast, independent of electronic appliances' working status, the powerline leakage is continuous and captured voltage at the ring antenna is stable [52].

We thus leverage this property of stability to extract the subtle signal variation for sensing. A straightforward method is to perform a subtraction operation between adjacent samples to remove the stable part of the signal. However, it does not work well because the body movement influence on the signals is in the form of multiplication instead of the addition, since the body movement will directly affect the physical characteristics of the "body-ring antenna", changing the antenna gain. In this work, we apply a self-multiplication operation together with a low-pass filter to remove the original 60 Hz component and the high-frequency component (120 Hz). The low-frequency component left is induced by target movement and can be extracted for sensing.

By addressing all the challenges, we design DancingAnt, the first ring antenna design together with human body as a key component to achieve body-empowered wireless sensing with leaked signals from powerlines. The cost of the whole system is less than \$10. It can sense human target movement to enable a large range of applications such as fall detection and sleep monitoring. The ring design makes DancingAnt convenient to wear, especially for the elderly. DancingAnt does not require any dedicated hardware for signal transmission. Its sensing process causes no interference to existing RF communication. Besides, the limited sensing coverage issue associated with conventional RF sensing caused by blockages is no longer a problem owing to the near-field nature of the proposed new sensing modality. To summarize, our main contributions are as below:

- We involve human body² into the receiver design to enable powerline sensing without requiring any dedicated transmitter or dedicated signal transmissions. We believe this is a promising new sensing modality which could trigger a large range of applications.
- We study the relationship between body movement and the signal variation both theoretically and experimentally. The experiment results match the theoretical analysis well. The observations obtained lay a foundation for exploiting powerline leakage for sensing purposes.
- We design signal processing methods to improve the sensing granularity, making fine-grained sensing possible with weak powerline RF leakages.
- We prototype a low-cost system, and comprehensively evaluate the performance of the system in varying scenarios. Promising results demonstrate that the leaked signals from the powerlines can be utilized for meaningful sensing such as falling detection and sleep monitoring.

²All the experiments conducted are IRB-approved by the host institute.

2 BACKGROUND

Powerline EMR. Owning to the widely adopted alternating current (50/60 Hz) for power supply, electromagnetic radiations (EMRs) are generated by powerlines in buildings. Such EMRs are pervasive in ambient environment as a result of the wide deployment of powerline infrastructure. While the EMRs generated by powerlines can cause unwanted interfering current in nearby circuits, it also produces audible noise known as mains hum in audio equipment [46]. Therefore, it is usually considered as "bad". In this paper, we propose to leverage the "bad" pervasive radiations for sensing purposes.

Bio-electricity of Human Body. Human body is mainly composed of body fluids, cells, bones, fat, and other materials, in which the body fluids and cell membranes contribute to the body's electric conductance and capacitance, respectively [41]. These bioelectric characteristics of the human body are fundamental to the working principles of magnetic resonance imaging in hospitals for taking detailed images of areas inside the body [48] and bioelectrical impedance analysis in measuring body composition [22]. Owning to the bioelectric characteristics of human body, human body can also be considered as a large-sized antenna for wireless signal reception. Although the performance of such a body antenna is not as good as antennas made of materials with high conductivity such as copper and aluminum, its relatively large size makes the body antenna meaningful in receiving some low-frequency signals [12, 33, 34]. Therefore, human body performs well in picking up the EMRs leaked from electric powerlines, which are also low-frequency signals. The powerline leakage is harmless for human health due to its extremely low frequency and low energy.

3 SENSING WITH POWERLINE EMR

In this section, we first analyze the preliminaries of sensing using powerline EMR. Then we study the impact of involving human body to receive the ultra-low frequency signal.

3.1 Preliminaries

Leveraging the near-field effect. Traditional wireless sensing systems typically employ high-frequency signals, such as Wi-Fi (e.g., 5 GHz) and mmWave (e.g., 24 GHz), which have relatively short wavelengths. These sensing technologies are developed based on the *far-field model* of electromagnetic radiation, which assumes that the distance between the target to sense and the radio frequency (RF) transceivers is much larger than the Fraunhofer distance d_F calculated as [1]

$$d_F = 2D^2/\lambda, \quad (1)$$

where D is the largest dimension of the antenna and λ is the wavelength of the signal. For example, in Wi-Fi based sensing, the Fraunhofer distance is around ten centimeters. In contrast, the proposed sensing with the electromagnetic

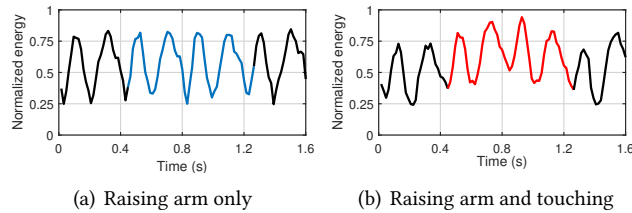


Figure 2: Using powerline EMR for sensing: (a) Short-term energy of signal when the target only raises his arm; (b) Short-term energy of signal when the target raises his arm while hands touching the metal plate.

radiation from the electric powerlines is conducted in the *near field* due to the extremely long wavelength (λ) of the leaked EMF signals ($3 \times 10^8 / 60 = 5000$ km).

Leveraging the electric field. Utilizing near-field signal for sensing raises a unique question regarding which electromagnetic field should be utilized for sensing, the electric field or the magnetic field. Given the proximity of the sensing target to the signal transmitter, we can also consider them as capacitive coupling or inductive coupling [52]. Different from EMR's far-field model in which the intensity ratio of the electric field and the magnetic field is constant, in near field, one of them typically dominates over the other [52]. Specifically, a higher voltage induces a stronger electric field, while a larger current induces a stronger magnetic field. The magnitude of the current variation in the powerline primarily depends on the status of the connected appliances, such that more working appliances lead to a larger current flow through the powerline. In contrast, the voltage remains relatively stable (110 V or 220 V). Although the voltage may fluctuate slightly when multiple appliances operate simultaneously, such changes are relatively small, ensuring proper appliance functionality. As a result, the electric field is typically more stable than the magnetic field. Given that signal stability is crucial for sensing, we have opted for the *electric field* in our system for sensing. Throughout the rest of the paper, we will refer to the received electric field of the EMR from the powerlines as “leaked signals”.

Traditional sensing model does not work. We conduct a preliminary experiment to show the infeasibility of utilizing leaked signals for traditional sensing. The setup consists of powerlines connected to five power sockets within the walls and four working appliances. We employ a 33 cm × 33 cm metal plate as the receiving antenna to capture the leaked signals. In conventional wireless sensing, the movements of human target affect the propagation path between the transmitter (e.g., powerline) and the receiver (e.g., metal plate). These movements cause variations of the received signals, which can be analyzed to infer the movements of the human target. Thus, the target (a person) is positioned 1.2 m from the receiver. We ask the target to raise his arm and use a GoPro

Hero9 camera to record the ground truth. The short-term energy [38] of the received signals is calculated and presented in Figure 2(a) with the signals during the movement process depicted in blue. It is challenging to discern any differences between the received signals when the target is stationary and when the target is raising his arm. The energy difference between the two signals is below 0.1%. The primary reason why target movement has little effect on the propagating signal is the ultra-low frequency of the signal, i.e., 50/60 Hz. Such leaked signal from the powerline has a much longer wavelength, i.e., five million meters, which allows it to easily diffract over obstacles smaller than its wavelength. Therefore, it is robust against propagation medium changes such as those caused by human targets in our experiment. Thus, conventional RF sensing model is ineffective in leveraging leaked signals from the powerline for sensing, and a new sensing model is needed for ultra-low frequency signals.

3.2 Human Body in the Loop of Antenna

Motivated by a recent study that leverages human body to improve the efficiency of energy harvesting [12], we hypothesize that if *the target's body is integrated into the loop of the receiving antenna*, the target's movement will have a significant impact on captured signals at the receiver. To verify our conjecture, we ask the target to touch the metal plate with his *left* arm and repeat the two aforementioned states: standing still and then raising his *right* arm. The short-term energy of detected signals is shown in Figure 2(b), where we can clearly see the energy change when the target raises his right arm, highlighted in red color.

Through this preliminary experiment, we discover that an effective way of enlarging the impact of target movements on the low-frequency signal is to have physical contact between the metal plate and the target's body. The underlying reason for this is that when human body is touching the metal plate, *the whole human body becomes part of the receiving antenna*. The body itself can collect wireless signals, as mentioned in Section 2. Thus when the metal plate and target body form the receiving antenna together, the target movement actually changes the physical form of this receiving antenna and then influences the received signals. Such a fact gives us the opportunity to leverage the leaked signals from the powerline for wireless sensing.

4 DANCINGANT: ANTENNA DESIGN

In this section, we describe the design of our body-empowered antenna. The antenna should satisfy several requirements: (i) convenient to carry; (ii) touch human body all the time; and (iii) achieve good performance in collecting leaked signals from powerline. Several aspects of the antenna are considered: matching resistance, thickness, size, and material.

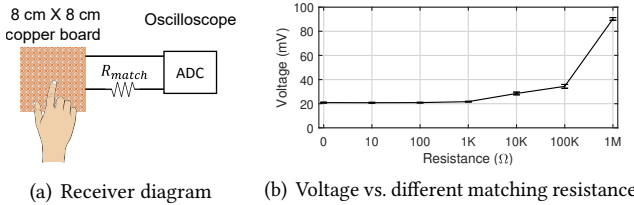


Figure 3: Validation of the matching resistance's influence: (a) Diagram of the receiving circuit with matching resistance; (b) Peak voltage of the received signals.

Matching impedance. We first investigate the effect of matching impedance between the receiving antenna and the data acquisition unit (e.g., ADC of the oscilloscope used in this experiment), as illustrated in Figure 3(a). The input impedance of the oscilloscope is set to $10\text{ M}\Omega$. The receiving antenna is an $8\text{ cm} \times 8\text{ cm}$ copper plate touched by the target finger to capture leaked signals. To represent the impedance of the matching network, we employ the resistance denoted as R_{match} since the reactance part is almost ignorable due to the low frequency of the leaked signal. To vary R_{match} , we utilize resistors of different values from $0\text{ }\Omega$ to $1\text{ M}\Omega$. We collect signals from the metal plate under varying matching resistances while the target sits still. We repeat the experiment twenty times for the same matching resistance. For each trial, we calculate the average peak voltage and standard deviation of the peak voltage. The results, as presented in Figure 3(b), show that larger matching resistance leads to better receiving performance, as indicated by the larger received signals. Specifically, the average peak voltage with $1\text{ M}\Omega$ matching resistance (90.3 mV) is four times larger than the average peak voltage with $1\text{ k}\Omega$ matching resistance (21.7 mV). To maximize the voltage captured at such “body-metal” antenna, we increase the matching resistance and observe that the largest voltage (569.8 mV) is obtained when there is no matching resistance, i.e., the matching resistance between the antenna and oscilloscope is close to infinite.³ Therefore, in the following experiments and the system design of DancingAnt, we maintain an open circuit to obtain a larger voltage for wireless sensing.

Thickness. Next, we study the influence of the metal plate’s physical parameters, i.e., thickness and size on the collected signals. To evaluate the effect of thickness, we first choose four copper plates with the same size ($15\text{ cm} \times 15\text{ cm}$) but different thicknesses, i.e., 0.05 mm , 0.4 mm , 0.8 mm , and 3.2 mm . We collect the signals from the metal plate with the index finger of left hand touching the metal. The detected peak voltages are 570.0 mV , 567.7 mV , 570.1 mV , and 569.5 mV , respectively. As a comparison, without the finger touching the metal, the average peak voltages are 65.4 mV , 74.1

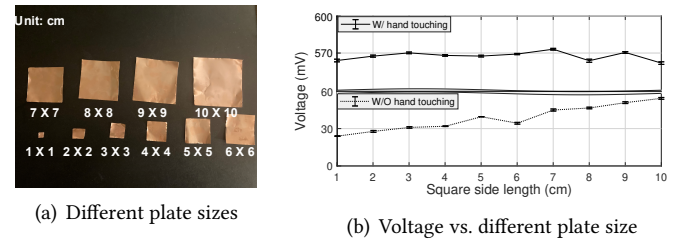


Figure 4: Validation of the metal plate size's influence: (a) Copper plates with different sizes; (b) Peak voltage of the received signals with different metal plate sizes.

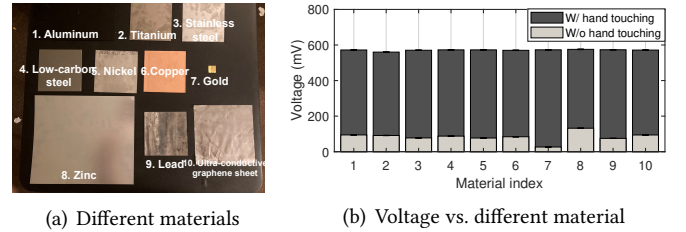
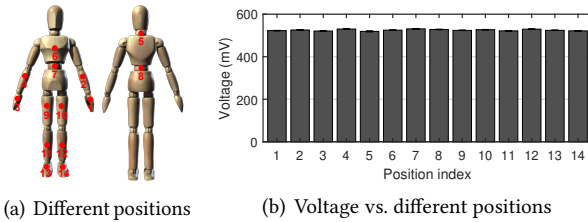


Figure 5: Validation of the metal plate material's influence: (a) Metal plates with different materials; (b) Peak voltage of the received signals.

mV , 84.0 mV , and 85.5 mV , respectively. The collected voltage from the copper plate without body touching increases with the thickness of the plate, which matches our intuition since a thicker metal plate can absorb more wireless energy in ambient environment. However, we can observe that the collected voltage is almost independent of the thickness when the copper plate is touched with the human body. This is because the contribution of human body to the received signal is much larger than the small metal. Therefore, the influence of the plate’s thickness on our body-empowered antenna is negligible.

Size. For validating the influence of the metal plate size, we conduct experiment with ten square-shaped copper plates with the same 0.05 mm thickness but different side lengths from 1 cm to 10 cm with a step size of 1 cm , as shown in Figure 4(a). We first placed these plates at the same position and collected the signals without any body touching. The average peak voltages of these plates, as shown in Figure 4(b), indicate that larger plates result in more signals being collected. Next, we collected the signals from the plates with the index finger of the left hand touching the plate. The results in Figure 4(b) indicate that there is almost no difference between the average peak voltage collected from copper plates of different sizes when they are connected to the human body. This is because now the main contributor of the receiving antenna is actually the human body, and the sizes of these copper plates are too small to have a significant impact on the overall receiving performance.

³Due to the electromagnetic coupling between the metal plate and the oscilloscope, the circuit is not completely open.

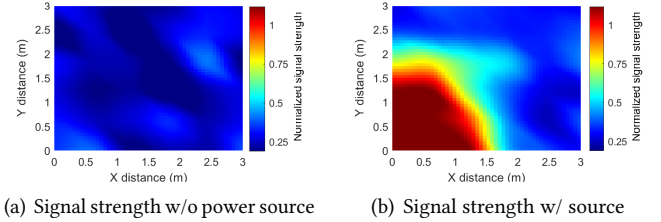


(a) Different positions (b) Voltage vs. different positions

Figure 6: Validation of position's influence: (a) Metal plates with different positions on the body; (b) Peak voltage of the received signals.

Material. We also study the effect of plate material on the collected signal. We select ten metal plates made of different materials: aluminum, titanium, stainless steel, low-carbon steel, nickel, copper, gold, zinc, lead, and ultra-conductive graphene, as shown in Figure 5(a). Following the same experiment procedure, we collect the signals from these metal plates both with and without body contact. The average peak voltages are shown in Figure 5(b). Our experiment results show that, when the metal plate is not in contact with the body, its size has a more significant impact on the received signals than the material, as indicated by the peak voltages collected from small gold (No.7), medium copper (No.6), and large zinc (No.8) plates. When the metal plate is in contact with the body, there is no significant difference in the voltage collected from plates made of different materials, due to the dominant influence of the human body on the received signals. This finding has important implications for our design, as copper, a commonly used material in electronic designs, can be used instead of expensive gold or hazardous lead.

Touching method. After analyzing the impact of the metal plate on the “body-metal” antenna, we proceed to investigate further the influence of the connection between the metal plate and human body. The first experiment aims to determine if cloth affects the received signals. The same human target touches the same copper plate with the same finger and posture but with cotton gloves for the first attempt and no gloves for the second. The peak voltage collected from the metal plate decreases by approximately 50% when there is a cloth between the body and metal plate. Hence, direct contact between the metal plate and the body skin is important to collect strong voltage for sensing. We then attach the same metal plate to different body parts of the target without any cloth, and the results in Figure 6(b) show little difference on the average peak voltage collected from metal plates at different positions (Figure 6(a)). Since the entire body is part of the receiving antenna, the connection point has little effect on the antenna’s performance, particularly in our system where the wavelength of the signals is much larger than the antenna size [1].



(a) Signal strength w/o power source (b) Signal strength w/ source

Figure 7: Signal strength with and w/o power source.

Body-ring antenna: final form. Based on the experiment results, the performance of the “body-metal” antenna is not affected by the size, thickness, material, or touching position of the metal plates. In other words, the metal strip serves as a connection point to the human body which is the actual “antenna”. Therefore, a thin copper strip is chosen to create a compact-sized ring antenna, as shown in Figure 13(b). This design is cost-effective and easily adaptable to various sizes and shapes. Moreover, the ring antenna is convenient for users to wear and maintain skin contact at all times, forming a “body-ring” antenna.

5 MODELING AND SOFTWARE DESIGN

5.1 Modeling the Effect of Body Movement on Signal Variation

We first study the impact of “body-ring” antenna movement on signal variation and establish the corresponding *body-empowered sensing* model. For typical RF antennas, changes in the antenna’s impedance, effective area, and distance from the transmitter can affect the received signals. To assess the influence of body movement on the received signals, we examine the changes in each of these parameters for the “body-ring” antenna. We acknowledge that other factors may influence the relationship between body movements and received signals. The derived model does not aim to exhaustively consider all the factors but serves as a starting point for the study in this direction.

Impedance. The impedance of an antenna plays a critical role in determining the matching loss between the antenna and the data acquisition unit. This, in turn, affects both the amplitude and phases of the received signal [1]. In the case of our “body-ring” antenna, the bioelectric characteristics of the human body result in changes in the impedance of the body. However, the impact of this impedance change on the received signal is negligible due to two factors. First, the resonant frequency of the human body for RF signals is in the range of tens of megahertz [27]. Thus, the impedance change has a minor effect on receiving low-frequency 50/60 Hz signals. Second, in our antenna design, an open circuit is used between the “body-ring” antenna and data acquisition device to enhance the voltage amplitude of received signals.

Distance from the transmitter. The physical form change of the antenna can alter the distance between the receiver and the signal source. While this effect is negligible for traditional RF signals like Wi-Fi, LoRa, and LTE, which have small antenna sizes and large distances from the signal source, it does affect the amplitude of the received signals in our model. To evaluate the impact of distance changes, we first collect signals picked up by our “body-ring” antenna without any signal source in a $3\text{ m} \times 3\text{ m}$ outdoor open area. The signal strengths at different positions are shown in Figure 7(a). Next, we place an AC power bank at the left-bottom corner of the area, i.e., point $(0\text{ m}, 0\text{ m})$ to charge a laptop with a constant output of 30 W. Using the same device, we collect signals at the “body-ring” antenna, and the signal strengths are shown in Figure 7(b). We can see that the signal strength is sensitive to distance, suggesting that target movement can induce signal amplitude variation.

Note that we use the power bank as the leakage source in outdoor scenarios to model the relationship between signal variation and body posture since there is no interference from other powerlines. In the rest of the paper, the leaked signal is from real indoor powerlines, reflecting real-world scenarios. Although the leaked signal from a power bank may not be exactly the same as that from powerlines, the derived model can still guide our sensing design because our focus is on the variation of signal amplitude associated with body postures. The frequencies of the two signals are similar, leading to similar signal variations.

Effective area. When the human target has different postures, the physical size of the “body-ring” antenna varies. Theoretically, a larger size of the body, indicating a larger antenna size, could receive more signals. To verify this, the target is asked to wear the designed ring antenna on the *left hand* and stand facing the signal source at point $(0\text{ m}, 1.5\text{ m})$. Then the target performs the following eight gestures, as illustrated in Figure 8(a), each for ten times. The normalized signal strengths under different postures are shown in Figure 8(b). We can see that postures 1-4 capture stronger signals due to the larger physical size of the “ring-body” antenna, which matches the theory that a larger physical size leads to larger received signals.

The result also shows that the target’s arm movements to 90° lead to stronger signal than arm movements to 180° due to a larger physical size. On the other hand, lower-body movements such as leg lifting and squatting decrease the body’s physical size, resulting in weaker signal compared to standing still. Additionally, the lying down posture exhibited the smallest signal due to its significantly smaller physical size. This unique property can be effectively harnessed for fall detection, which will be elaborated in Section 7. The relatively small signal variation resulted from other postures

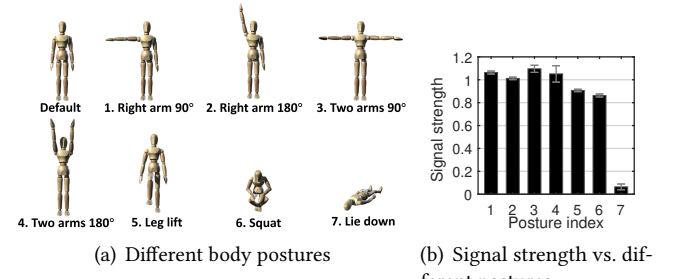


Figure 8: Validation of the body postures influence: (a) Diagrams of different body postures; (b) Signal strength of the received signals with different body postures.

can also be leveraged to guide the proposed body-empowered sensing in the following subsections.

5.2 Sensing Signal Extraction

Our near-field sensing model relies solely on amplitude changes, unlike conventional far-field models that utilize both amplitude and phase variations for sensing. While different body postures induce varying signal strengths, certain postures, such as upper body movements, generate signal variations less than 5% based on our measurements. The small variation makes it challenging to distinguish these postures. For instance, consider the scenario where the target raises his right arm to the side. We extract the detected signal variation resulted from the movement using traditional signal processing methods, i.e., envelope detection and short-term energy detection. The processed signals are depicted in Figure 9. We can hardly see any signal changes from the two methods since the signal variation is buried by noise.

To boost the sensing resolution of collected signals, we exploit a distinct property of leaked signals from the powerline. Specifically, the leaked wireless signals exhibit stability and continuity. This is in contrast to conventional RF signals used for communication, such as Wi-Fi, which varies all the time [47]. Furthermore, the leaked signals from the powerline are consistent 60 Hz sine wave signals. Since we capture the voltage instead of the current in the near field, the signal amplitude is also relatively stable, irrespective of the electronic appliance usage in the environment.

Besides the stability of the leaked signals in both amplitude and frequency, the frequency of the signal variation caused by motions is smaller than the frequency of the leaked signals, i.e., 50/60 Hz. The target motion influences the leaked signals in a multiplication way since the target motion changes the physical form of the body-ring antenna, influencing the antenna gain. Based on these properties, we can treat the target motion’s influence on the leaked signals as the process of amplitude modulation in communication [54] as

$$x(t) = m(t) \cos(\omega t), \quad (2)$$

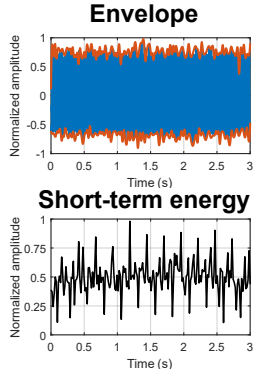


Figure 9: Existing signal processing.

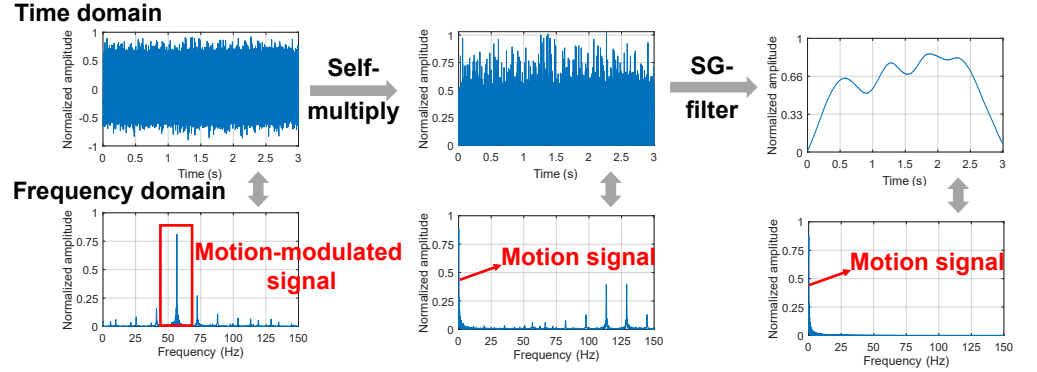


Figure 10: Proposed signal processing of considering the received signals as modulated signals.

where $m(t)$ is the motion signal (message signal) in the low-frequency band, $\cos(\omega t)$ is the leaked signal (carrier signal), and $x(t)$ is the received signals at the “body-ring” antenna.

To extract the motion signal from the received signal, we need to perform similar processing as that in amplitude demodulation in communication, i.e., multiplying the received signals with the carrier signals and filtering it with a low-pass filter to demodulate the message signal. Instead of imitating the demodulation in signal processing, we find that multiplying the received signal by itself instead of the carrier signal (uninfluenced leaked signals) would further increase the sensing sensitivity to target motion as

$$\begin{aligned} y(t) &= m(t) \cos(\omega t) * m(t) \cos(\omega t), \\ &= m^2(t) \left(\frac{1 + \cos(2\omega t)}{2} \right), \end{aligned} \quad (3)$$

where $y(t)$ is the resulted signal of self-multiplication. The signal variation caused by motion $m(t)$ is squared during the self-multiplication process, compared with signals without any movements. Besides, such a process increases the signal processing speed since there is no need to find synchronized carrier signals. After using the low-pass filter, i.e., Savitzky-Golay filter, to remove the high-frequency part $\cos(2\omega t)$, we can extract the motion signals. Figure 10 shows the collected signals when the target raises his right arm side up in both time and frequency domains using the proposed signal processing method. We can observe that the low-frequency motion signal is successfully extracted from the large leaked signals in both time and frequency domains.

5.3 Body Gesture Recognition

After extracting motion signals from the received signals, we classify them into different types of gestures based on the established body-empowered sensing model. For clarity, we term the extracted motion signals as data samples in this section. Besides, we only consider challenging scenarios for gesture classification when there are no nearby signal sources (powerines and electronic appliances). In scenarios

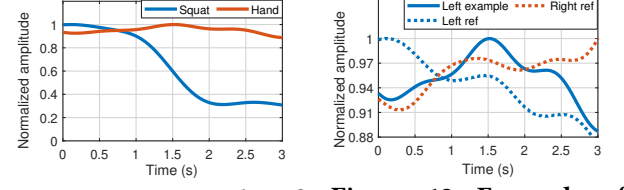


Figure 11: Example of coarse guidance.

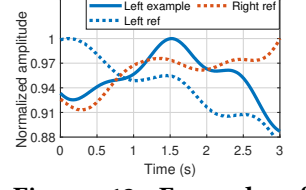


Figure 12: Example of fine guidance.

where the target is close to signal sources, the larger signal variations make gesture classification much easier.

Step 1: Dividing into different groups. We first use the established model to preliminarily classify the collected data samples into different groups of gestures based on three metrics: 1) the ratio between the maximum data point and the minimum data point (i.e., motion scale), 2) the ratio between the total signal variation compared with the beginning data point (i.e., intensity of the motion), and 3) the duration of the signal variation (i.e., motion duration). Taking the first metric as an example. We can easily classify squatting and hand movement as shown in Figure 11. The signal change caused by squatting is much larger than that caused by hand movement since the posture of squatting receives much fewer leaked signals.

Step 2: Fine guidance. The extracted samples are further classified within each group. To do so, a set of N reference samples ($S_{\text{ref}}(1, \dots, N)$) are collected for each group. The dynamic time warping (DTW) technique [36] is then employed to compare the DTW distances between the received sample (s_c) and each of the reference samples ($S_{\text{ref}}(i), i \in N$). The gesture corresponding to the reference sample with the smallest DTW distance is chosen as the classification result. However, simply using the DTW below

$$\arg \min_{i \in N} \text{DTW}(s_c, S_{\text{ref}}(i)) \quad (4)$$

can result in incorrect classification in the presence of hardware/environmental noise. For instance, as shown in Figure 12, the DTW-based classification method outputs an

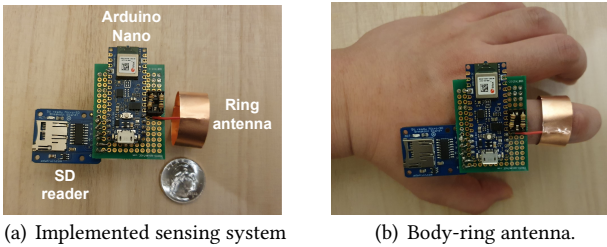


Figure 13: Implementation of the DancingAnt system.

incorrect gesture result. The blue solid line represents a sample of the target performing a left swiping with the right hand, the blue dotted line represents the reference sample of performing a left swiping with right hand, and the red dotted line represents the reference sample of performing a right swiping with the right hand. The DTW distance between the blue solid line and blue dotted line is 60.14, larger than the distance between the blue solid line and red dotted line, which is 50.20. Consequently, the DTW algorithm incorrectly classifies this sample as a right swiping.

However, it is observed that the endpoint of the blue solid line is smaller than its startpoint, a condition also true for the blue dotted line, but not for the red dotted line. This is because the starting posture for left swiping with the right hand has a larger body size than the ending posture. As discussed in Section 5.1, a larger body size results in more leaked signals being collected. Conversely, the body size of the beginning posture for right-swiping with the right hand is smaller than the ending posture.

So we define a function $P(s)$ to indicate whether the motion signal of the starting posture (s_{start}) is greater or smaller than that of the ending posture (s_{end})

$$P(s) = \begin{cases} 0, & \text{if } s_{\text{start}} \geq s_{\text{end}}, \\ 1, & \text{if } s_{\text{start}} < s_{\text{end}}. \end{cases} \quad (5)$$

Finally, we design a classification algorithm that combines the DTW distance and the start-end posture difference between the collected sample and the reference samples. Specifically, the algorithm minimizes the sum of the DTW distance between collected sample s_c and each reference sample $S_{\text{ref}}(i)$ in N , and absolute difference between the start-end posture difference of s_c and $S_{\text{ref}}(i)$ weighted by a parameter α

$$\arg \min_{i \in N} (\text{DTW}(s_c, S_{\text{ref}}(i)) + \alpha |P(s_c) - P(S_{\text{ref}}(i))|). \quad (6)$$

This classification algorithm is particularly useful for gestures that have different starting and ending postures, such as up-swiping with the right hand and down-swiping with the left hand, sitting down on a chair, and standing up from a chair.

6 IMPLEMENTATION

In this section, we present the implementation details of our body-empowered sensing system. As shown in Figure 13(a), we use a copper strip with a thickness of 0.05 mm to design the ring antenna, and use an Arduino Nano board to collect data from the ring. The data is stored in an SD card and further transferred to a laptop with an Intel i7 CPU and 16 GB memory for signal processing. Besides, we can also leverage the built-in Bluetooth® Low Energy (BLE) module to transfer information without incurring any additional costs. The power consumption of Bluetooth module for data transmission is approximately 0.1 W. We find that turning on/off the Bluetooth module at the receiver has no impact on the 50/60 Hz signals because these two types of signals have different frequencies. Even though the DC power increases when the BLE module is switched on, we utilize the signal variation (i.e., relative signal power) instead of absolute signal power for sensing. We also design a passive voltage divider consisting of two 10 MΩ resistors to collect the leaked signals from the powerline. The self-made ring antenna is very cheap, i.e., less than 10 dollars. The users can wear the whole system on their fingers as shown in Figure 13(b). If we design our own PCB to replace the Arduino Nano board for signal processing, the size can be reduced to around 1 cm × 2 cm.

Note that we do not require any additional transmitters⁴ but only utilize the leaked signals from the powerline that already exists in our daily life. As the powerline leakage is small and extremely low-frequency, exposure to this leakage does not cause any health issues. We utilize an open circuit to amplify the voltage value, accompanied by an infinitely high resistor value. As a result, the energy absorbed by the body is negligible. All the experiments were IRB-approved by our institute.

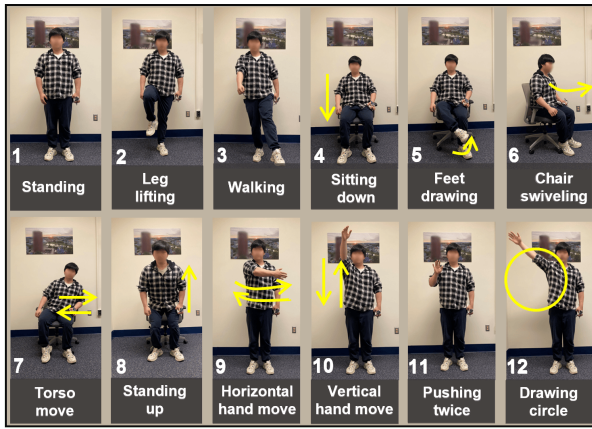
7 EVALUATION

We first evaluate the performance of DancingAnt on gesture classification and compare it with Wi-Fi sensing [61] in terms of sensing coverage. We also conduct comprehensive experiments to evaluate the robustness of DancingAnt under different environment conditions. Furthermore, we present two case studies, i.e., sleep monitoring and fall detection, to demonstrate the applicability of powerline sensing.

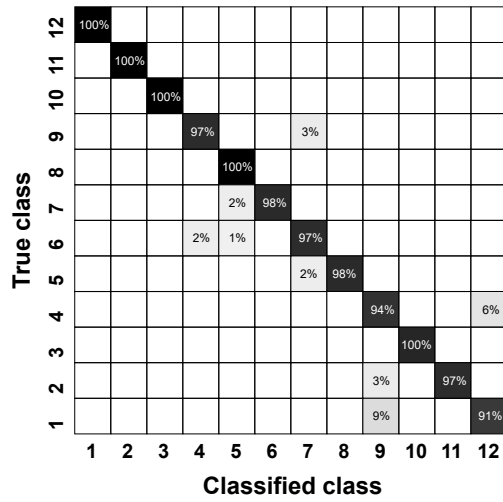
7.1 Sensing Body Gestures/Postures

To evaluate the gesture classification accuracy of DancingAnt, we employ 12 different gestures as shown in Figure 14(a). For each gesture, we run the experiments 100 times. We conduct experiments in a typical apartment as shown in Figure 15(a).

⁴We do need communication signals such as Wi-Fi and Bluetooth to transfer the signal samples to a laptop or a smartphone for local processing. This Bluetooth/Wi-Fi signal is not a sensing signal but a communication signal.



(a) Illustration of the investigated 12 body postures



(b) Experiment result

Figure 14: The evaluated 12 different body postures.

During the experiments, the target wears DancingAnt on the index finger of the left hand. Note that even though the gestures do not involve the movement of the left hand wearing the DancingAnt, we can still sense the gestures. In other words, *by simply wearing DancingAnt on one finger, we can efficiently sense the whole body movement*.

Figure 14(b) shows that the average classification accuracy is 97.7%. From the experiment results, we observe that it is easier to identify the gestures involving leg movements, such as lifting leg, walking, and feet drawing while sitting. Moreover, the gestures with whole body movement (i.e., 4, 6, 7, 8) and the gestures only with hand movement (i.e., 9, 10, 11, 12) induce very different signal variation amplitudes. As a result, we can achieve a 100% classification accuracy in distinguishing the gestures between these two groups.

7.2 Experiments in Different Environments

We conduct experiments in three different environments, i.e., an apartment, a lab and an office as shown in Figure 15(a) ~ 15(c), to evaluate the robustness of DancingAnt. In each environment, we uniformly select 10 locations and ask the target to perform four gestures, i.e., stand, walk, horizontal hand move, and vertical hand move at each location. For each gesture at each location, we repeat the experiments 10 times. Figure 15(d) shows that the classification accuracies in these three environments are 96.25%, 94.75%, and 97.75%, respectively. These results demonstrate the robustness of DancingAnt in different environments.

7.3 Comparison with Wi-Fi Sensing in Terms of Sensing Coverage

We compare DancingAnt with the state-of-the-art Wi-Fi sensing system, i.e., *FarSense* [61], in terms of sensing coverage. The sensing coverage is defined as the area where the gesture of target can be sensed. For *FarSense*, we employ Gigabyte GB-BXBT-1900 Mini PC and Intel Wi-Fi 5300 card to set up the transmitter and receiver. Figure 16 shows the deployment of Wi-Fi transmitter and receiver. We use one antenna at the transmitter, and equip the receiver with two antennas to perform the signal ratio operation for a longer Wi-Fi sensing range [61]. The distance between two antennas at the receiver is half wavelength i.e., 2.9 cm at the central frequency of 5.24 GHz.

To measure the sensing coverage, we divide the whole apartment into 50 cm × 50 cm grids and the target performs one gesture, i.e., horizontally moving the right hand, in each grid. As shown in Figure 16, the sensing coverage of *FarSense* is much smaller because the Wi-Fi signals get significantly attenuated after penetrating walls. On the other hand, DancingAnt achieves a much larger sensing coverage. This is one key advantage of our system. We utilize the leaked signals from the pervasive powerlines to sense human motions, which can cover the whole apartment without being affected by walls.

7.4 Robustness

We also evaluate whether DancingAnt is affected by the working status of appliances, surrounding interference, floor type, shoes, and skin moisture.

Impact of appliance working status. We conduct experiments in an apartment and divide the appliances inside into five groups based on their positions as shown in Figure 15(a). We set up six appliance working status in the experiments. *Status 1*: we turn off the appliances in all the areas. *Status 2*: we only turn on the appliances in area 1, and keep the appliances in other areas switched off. *Status 3*: we turn on the appliances in area 1 and area 2. *Status 4*: we turn on the

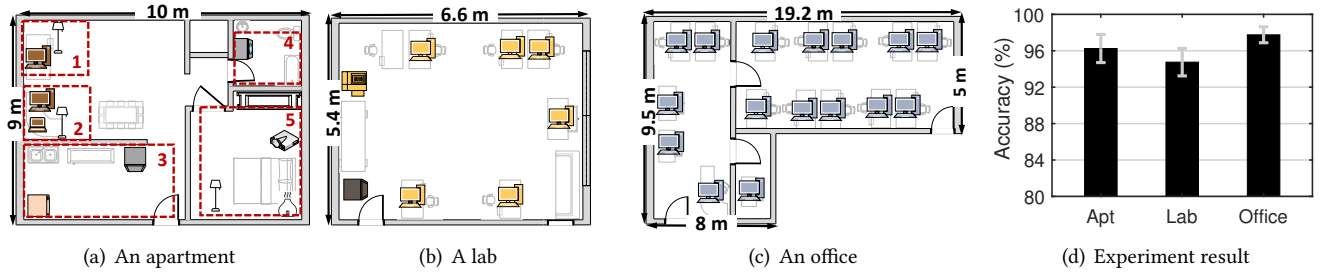


Figure 15: Experiments in three environments.

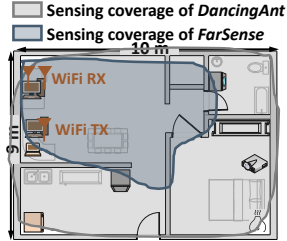


Figure 16: Sensing coverage: comparison with Wi-Fi.

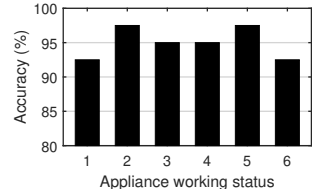


Figure 17: Robustness to appliance usage.

appliances in area 1 ~ area 3. *Status 5*: we turn on the appliances in area 1 ~ area 4. *Status 6*: we turn on the appliances in all the areas.

For each status, the target stands in front of the computer in area 1 and performs four gestures: standing, walking, horizontal hand movement, and vertical hand movement. Each gesture is repeated 10 times. As shown in Figure 17, we can observe that all the classification accuracies are higher than 92%. The slight fluctuations in classification accuracies arise from the fact that gestures performed by the same target at different timestamps are not perfectly identical. Therefore, DancingAnt works well under different appliance working statuses.

Impact of interference. Now we study the impact of surrounding interferer's movement on the sensing performance. We conduct experiments with one target and one interferer as shown in Figure 18(a). We vary the distance between target and interferer from 0 m to 3 m at a step size of 0.5 m. When the target and interferer are side-by-side, the distance between them is 0 m. For each target-interferer distance, the target performs four gestures, i.e., standing, walking, horizontal hand move, and vertical hand move, while the interferer moves randomly. The experiment results are shown in Figure 18(b). As we can see, when the target-interferer distance is larger than 0 m, the classification accuracies are higher than 95%. When the target and interferer are side-by-side, the classification accuracy slightly decreases to around 92.5%. These experiment results demonstrate that DancingAnt is robust against surrounding interference.

Impact of touching. We find that physical contact between a target wearing DancingAnt and another person

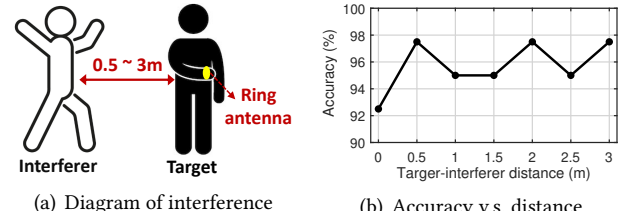
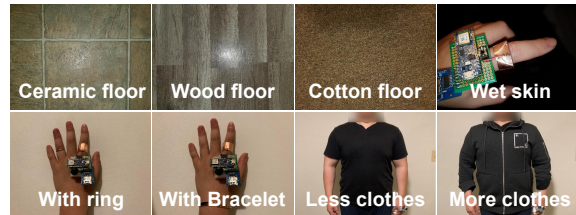


Figure 18: Robustness to surrounding interference.

affects the received signal's amplitude, leading to potential degradation of the sensing accuracy. Interestingly, we find that as long as only one person is performing gestures, DancingAnt can still effectively extract the gesture information when one person is touching another person. In our experiment setup, one person wore the proposed system and kept stationary. A second person touched the first person while performing four gestures: standing, walking, horizontal hand move, and vertical hand move. Impressively, the achieved gesture recognition accuracy is 92.3%. The experiment results present an interesting application scenario of the proposed sensing modality: although not wearing the device, one individual's movements and gestures can still be accurately sensed through touch-based interactions when another person is wearing the system.

Impact of other factors. We first evaluate the impact of floor type, and then investigate the impact of skin moisture. In addition, we study the effect of wearing metal jewelry, the presence of shoes, and the quantity of clothing. All the experiments are conducted with four gestures i.e., standing, walking, horizontal hand move, and vertical hand move. In the first experiment, the target wearing shoes stands on three types of floors, i.e., ceramic floor, wood floor, and cotton floor as shown in Figure 19(a). As shown in Figure 19(b), the classification accuracies are higher than 95%, demonstrating the floor type has little impact on the sensing performance of DancingAnt. Second, we evaluate the system performance in two scenarios: (i) the target's fingers are wet and (ii) the entire body of the target is wet (e.g., during a shower). Surprisingly, the classification accuracies are roughly the same in these two scenarios. Third, when the target does not wear shoes and stands on the cotton floor, the achieved accuracy is very close to that in the scenario when the target wears



(a) Types of different floors and body conditions

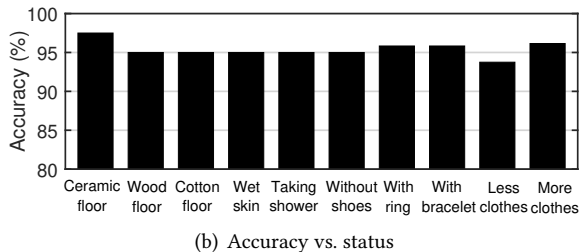


Figure 19: Robustness to floor types & body conditions.

shoes and stands on the same cotton floor. Finally, we ask the target to wear different metal jewelries such as ring and bracelet and change the quantity of clothing. As shown in Figure 19(b), the accuracy does vary with these factors, but the variation is quite small.

7.5 Case Study

Lastly, we present two case studies that are very important in elderly care, i.e., sleep monitoring and fall detection.

Sleep monitoring. Sleep posture monitoring is important for detecting apnea events, tracking the progression of Parkinson's disease, and even alerting epilepsy patients on potential fatal sleep postures [24, 60]. Different from previous works [24, 60] which monitor the sleep posture for only one target, we conduct experiments in a challenging scenario, i.e., two people (one couple) sleeping in one bed as shown in Figure 21. Both the two targets wear DancingAnt, naturally change their postures during sleeping. The sleeping posture change mainly involves a) Back to Side; b) Side to Stomach; and c) Stomach to Back. The classification accuracies for User A and User B are shown in Figure 20(b) and Figure 20(c), respectively. We can see that the accuracies are higher than 90%, demonstrating the effectiveness of our method.

Fall detection. Fall is recognized as one of the most frequent accidents among the elderly, and fall detection can effectively prevent or lessen injuries caused by falls [50]. Different from previous works which mainly detect whether the fall happens [18, 50], DancingAnt can also identify three different fall postures, i.e., fall forward, fall backward, and fall on the side. In our experiments, the target wears the proposed ring device and randomly falls on the cotton floor.

Figure 21(a) displays the classification accuracies for three fall postures, which are 100%, 80%, and 100% respectively.

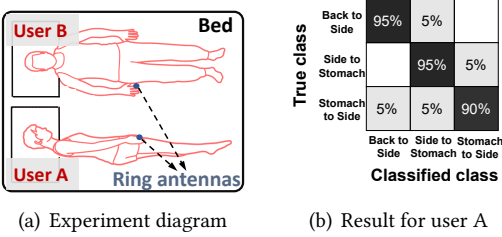
We also estimate the time duration between falling down and standing up, which is also a critical parameter in elderly fall detection [50]. DancingAnt records the timestamp of sudden signal changes induced by falling down and standing up, and estimates the time interval. The ground truth is obtained from a Go-Pro Hero9 camera. Figure 21(b) shows the difference between the estimated time duration and the ground truth. We can see that DancingAnt can estimate the time duration between falling down and standing up with an error below one second for all three types of falls.

8 DISCUSSION

Difference between the proposed approach and IMU sensors. DancingAnt differs from IMU-based sensors in both underlying principle and sensing performance. IMU sensors convert human motion information into electrical signals and can only sense the movement of the body part they are attached to. For example, an IMU sensor attached to the finger can only capture finger motions but not the leg or head motions. In contrast, DancingAnt utilizes the entire human body as a receiving antenna for electromagnetic wave reception and infers body motions by analyzing variations of the collected signals. Thus, DancingAnt is capable of sensing the motions of the entire body, regardless of the location the sensor is attached to. Even if the ring is worn on the finger, it can still sense the motion of other body parts.

Location diversity. The amplitude of the leaked signal indeed varies across target locations. However, we care about the relative signal amplitude variation pattern for human sensing rather than the absolute signal amplitude. Therefore, even though the absolute leakage amplitudes vary with target locations, the corresponding amplitude variation patterns are still similar which can be utilized for cross-location sensing. Our findings indicate that large movements such as walking exhibit stable and distinctive signal variation patterns, while small movements such as hand gestures are prone to be influenced by the target locations. Moreover, when the user is close to leaked signal sources, additional factors such as target-source distance also affect the signal variation pattern. We believe a machine learning method equipped with the capability of transfer learning could tackle this concern and we leave this for future work.

Calibration for different positions. The current system needs a one-time calibration to classify gestures, especially when users are close to signal sources. Variations on motion signal patterns due to distance change between users and signal sources can affect the signal pattern. We believe simultaneous localization and mapping based on powerline leakage [31] can be used to determine signal source locations and user position, eliminating the need for calibration.



(a) Experiment diagram

(b) Result for user A

(c) Result for user B

Figure 20: Sleeping monitoring.

Calibrations for different people. The Dynamic Time Warping (DTW) method used in the current system is per-user trained. Through our experiments, we notice that individuals with smaller body sizes tend to collect less leaked energy from the powerline. Moreover, different users may perform the same posture in different ways, thus per-user training remains necessary to achieve a high accuracy. We believe a machine learning method equipped with the capability of transfer learning [14] can address this issue.

Complicated gesture sensing. The current dataset contains relatively simple gestures, allowing the system to use traditional signal processing methods such as DTW for classification. Besides, our system cannot sense very fine-grained motions such as human respiration and heartbeat due to the minute change of the signal. We believe a larger set of poses/gestures and more complicated poses/gestures can be handled with lightweight machine learning models.

9 RELATED WORK

On-body sensors. IMU-based on-body sensors have gained a significant amount of attention on sensing target movements [16, 17, 21]. Researchers have employed on-body sensors for a variety of applications including fall detection [2, 19], sleep monitoring [4, 23], and activity recognition [6, 35]. DancingAnt introduces a different modality for on-body sensing. Unlike conventional on-body sensors that can only detect movements of specific body parts where the sensors are attached, DancingAnt has the capability to sense movements of the entire body.

Wireless sensing. Wireless signals have been extensively studied for sensing in recent years. Various signals such as Radar [62, 65], Wi-Fi [37, 51], acoustic [64], RFID [56], and light [13, 32], have been utilized for this purpose. Wireless sensing has enabled a large range of applications including activity recognition [42, 63], fall detection [49, 58], and sleep monitoring [29, 59]. Some recent works further utilize video-based RF simulation [5] and unsupervised representation learning framework [43] to reduce and even remove the training load in wireless sensing. Although promising, these modalities have fundamental limitations, such as requiring dedicated devices or signals [13, 32, 62], dead zones [37, 56], and interfering with existing communication [57]. In this

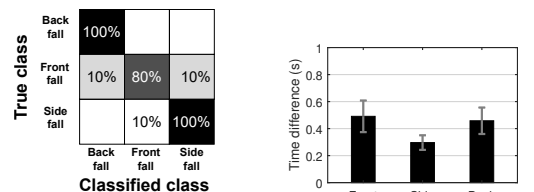


Figure 21: Fall detection.

study, we propose a new sensing modality based on powerline leakage which can efficiently bypass these issues.

Human body as an antenna. Human body is widely exploited as the electromagnetic antennas [27, 33, 34]. Owning to its relatively large physical size, human body is utilized as a low-frequency monopole antenna for communication [34] and energy harvesting [12, 27]. A similar existing work, Humantenna [10], utilizes the powerline leaked signals to conduct sensing with the help of human body. Differently, we design a compact-sized ring antenna to involve, and establish a body-empowered sensing model to guide sensing without complicated data training.

Powerline leaked signals. Leaked signals from the powerline have been exploited for different applications [11, 40, 44]. Researchers utilize the powerline EMR's unique spatial distribution for simultaneous localization and mapping [31] and touching detection [11]. The leakage is also leveraged for runtime clock verification [28] and clock synchronizing[40] owing to its temporal stability. Besides, recent work also proposes to use a stick-on capacitive energy harvester to collect the leaked signals to power IoT devices [15].

Electric field sensing. Researchers have discovered that electric charge in human body can vary with body movements and utilized this change to capture body motion [3, 9, 25]. Our work is different from these works as human body is considered as part of the antenna to receive powerline leakage for sensing.

10 CONCLUSION

In this work, we propose a new sensing modality, i.e., instead of influencing the propagation medium of wireless signal for sensing, we make human body part of the receiving antenna and extract the influence of human movement on the antenna for sensing. The basic principle is that human body can capture the leaked signals from powerline, and the amount of collected signal energy is affected by body postures. To enable this sensing, a ring-like antenna is designed to involve the human body in the loop of signal reception. The proposed system is used to realize several representative applications, including gesture recognition, sleep monitoring and fall detection.

REFERENCES

- [1] Constantine A Balanis. 2015. *Antenna theory: analysis and design*. John Wiley & Sons.
- [2] Patricia Bet, Paula C Castro, and Moacir A Ponti. 2019. Fall detection and fall risk assessment in older person using wearable sensors: A systematic review. *International journal of medical informatics* 130 (2019), 103946.
- [3] Sizhen Bian, Vitor F Rey, Peter Hevesi, and Paul Lukowicz. 2019. Passive capacitive based approach for full body gym workout recognition and counting. In *2019 IEEE International Conference on Pervasive Computing and Communications (PerCom)*. IEEE, 1–10.
- [4] Stanislav Bobovych, Fahad Sayeed, Nilanjan Banerjee, Ryan Robucci, and Richard P Allen. 2020. RestEaZe: Low-power accurate sleep monitoring using a wearable multi-sensor ankle band. *Smart Health* 16 (2020), 100113.
- [5] Hong Cai, Belal Korany, Chitra R Karanam, and Yasamin Mostofi. 2020. Teaching rf to sense without rf training measurements. *Proceedings of the ACM on Interactive, Mobile, Wearable and Ubiquitous Technologies* 4, 4 (2020), 1–22.
- [6] Liming Chen, Jesse Hoey, Chris D Nugent, Diane J Cook, and Zhiwen Yu. 2012. Sensor-based activity recognition. *IEEE Transactions on Systems, Man, and Cybernetics, Part C (Applications and Reviews)* 42, 6 (2012), 790–808.
- [7] Zicheng Chi, Xin Liu, Wei Wang, Yao Yao, and Ting Zhu. 2020. Leveraging ambient lte traffic for ubiquitous passive communication. In *Proceedings of the Annual conference of the ACM Special Interest Group on Data Communication on the applications, technologies, architectures, and protocols for computer communication*. 172–185.
- [8] Mostafa Zaman Chowdhury, Md Shahjalal, Shakil Ahmed, and Yeong Min Jang. 2020. 6G wireless communication systems: Applications, requirements, technologies, challenges, and research directions. *IEEE Open Journal of the Communications Society* 1 (2020), 957–975.
- [9] Gabe Cohn, Sidhant Gupta, Tien-Jui Lee, Dan Morris, Joshua R Smith, Matthew S Reynolds, Desney S Tan, and Shwetak N Patel. 2012. An ultra-low-power human body motion sensor using static electric field sensing. In *Proceedings of the 2012 ACM conference on ubiquitous computing*. 99–102.
- [10] Gabe Cohn, Daniel Morris, Shwetak Patel, and Desney Tan. 2012. Humantenna: using the body as an antenna for real-time whole-body interaction. In *Proceedings of the SIGCHI Conference on Human Factors in Computing Systems*. 1901–1910.
- [11] Gabe Cohn, Daniel Morris, Shwetak N Patel, and Desney S Tan. 2011. Your noise is my command: sensing gestures using the body as an antenna. In *Proceedings of the SIGCHI conference on human factors in computing systems*. 791–800.
- [12] Minhao Cui, Qing Wang, and Jie Xiong. 2022. Bracelet+: Harvesting the Leaked RF Energy in VLC with Wearable Bracelet Antenna. In *Proceedings of the 20th ACM Conference on Embedded Networked Sensor Systems*. 250–262.
- [13] Nathaniel Faulkner, Fakhrul Alam, Mathew Legg, and Serge Demidenko. 2019. Smart wall: Passive visible light positioning with ambient light only. In *2019 IEEE International Instrumentation and Measurement Technology Conference (I2MTC)*. IEEE, 1–6.
- [14] Zhongzheng Fu, Xinrun He, Enkai Wang, Jun Huo, Jian Huang, and Dongrui Wu. 2021. Personalized human activity recognition based on integrated wearable sensor and transfer learning. *Sensors* 21, 3 (2021), 885.
- [15] Manoj Gulati, Farshid Salemi Parizi, Eric Whitmire, Sidhant Gupta, Shobha Sundar Ram, Amarjeet Singh, and Shwetak N Patel. 2018. CapHarvester: A stick-on capacitive energy harvester using stray electric field from AC power lines. *Proceedings of the ACM on Interactive, Mobile, Wearable and Ubiquitous Technologies* 2, 3 (2018), 1–20.
- [16] Abdu Gumaei, Mohammad Mehedi Hassan, Abdulhameed Alelaiwi, and Hussain Alsalmi. 2019. A hybrid deep learning model for human activity recognition using multimodal body sensing data. *IEEE Access* 7 (2019), 99152–99160.
- [17] Jajack Heikenfeld, Andrew Jajack, Jim Rogers, Philipp Gutruf, Lei Tian, Tingrui Pan, Ruya Li, Michelle Khine, Jintae Kim, and Juanhong Wang. 2018. Wearable sensors: modalities, challenges, and prospects. *Lab on a Chip* 18, 2 (2018), 217–248.
- [18] Yuqian Hu, Feng Zhang, Chenshu Wu, Beibei Wang, and KJ Ray Liu. 2021. DeFall: Environment-independent passive fall detection using WiFi. *IEEE Internet of Things Journal (IoTJ)* 9, 11 (2021), 8515–8530.
- [19] Faisal Hussain, Fawad Hussain, Muhammad Ehatisham-ul Haq, and Muhammad Awais Azam. 2019. Activity-aware fall detection and recognition based on wearable sensors. *IEEE Sensors Journal* 19, 12 (2019), 4528–4536.
- [20] Wenjun Jiang, Hongfei Xue, Chenglin Miao, Shiyang Wang, Sen Lin, Chong Tian, Srinivasan Murali, Haochen Hu, Zhi Sun, and Lu Su. 2020. Towards 3D human pose construction using wifi. In *26th Annual International Conference on Mobile Computing and Networking (MobiCom)*. ACM, 1–14.
- [21] Théo Jourdan, Noëlie Debs, and Carole Frindel. 2021. The contribution of machine learning in the validation of commercial wearable sensors for gait monitoring in patients: a systematic review. *Sensors* 21, 14 (2021), 4808.
- [22] Robert F Kushner. 1992. Bioelectrical impedance analysis: a review of principles and applications. *Journal of the American college of nutrition* 11, 2 (1992), 199–209.
- [23] Shinjae Kwon, Hojoong Kim, and Woon-Hong Yeo. 2021. Recent advances in wearable sensors and portable electronics for sleep monitoring. *Iscience* 24, 5 (2021).
- [24] Derek Ka-Hei Lai, Li-Wen Zha, Tommy Yau-Nam Leung, Andy Yiu-Chau Tam, Bryan Pak-Hei So, Hyo-Jung Lim, Daphne Sze Ki Cheung, Duo Wai-Chi Wong, and James Chung-Wai Cheung. 2023. Dual ultra-wideband (UWB) radar-based sleep posture recognition system: Towards ubiquitous sleep monitoring. *Engineered Regeneration* 4, 1 (2023), 36–43.
- [25] Shane Lambert, Haitao Lu, Zane Shreve, Yi Zhan, AKM Jahangir Alam Majumder, and Gokhan Sahin. 2020. Low-powered wearable motion detecting system using static electric fields. *IET Cyber-Physical Systems: Theory & Applications* 5, 1 (2020), 31–38.
- [26] Dong Li, Shirui Cao, Sungsoon Ivan Lee, and Jie Xiong. 2022. Experience: practical problems for acoustic sensing. In *Proceedings of the 28th Annual International Conference on Mobile Computing And Networking*. 381–390.
- [27] Jiamin Li, Yilong Dong, Jeong Hoan Park, and Jerald Yoo. 2021. Body-coupled power transmission and energy harvesting. *Nature Electronics* 4, 7 (2021), 530–538.
- [28] Yang Li, Rui Tan, and David KY Yau. 2017. Natural timestamping using powerline electromagnetic radiation. In *Proceedings of the 16th ACM/IEEE International Conference on Information Processing in Sensor Networks*. 55–66.
- [29] Chen Liu, Jie Xiong, Lin Cai, Lin Feng, Xiaojiang Chen, and Dingyi Fang. 2019. Beyond respiration: Contactless sleep sound-activity recognition using RF signals. *Proceedings of the ACM on Interactive, Mobile, Wearable and Ubiquitous Technologies* 3, 3 (2019), 1–22.
- [30] Jian Liu, Hongbo Liu, Yingying Chen, Yan Wang, and Chen Wang. 2019. Wireless sensing for human activity: A survey. *IEEE Communications Surveys & Tutorials* 22, 3 (2019), 1629–1645.
- [31] Chris Xiaoxuan Lu, Yang Li, Peijun Zhao, Changhao Chen, Linhai Xie, Hongkai Wen, Rui Tan, and Niki Trigoni. 2018. Simultaneous localization and mapping with power network electromagnetic field. In *Proceedings of the ACM International Conference on Mobile Computing*

- and Networking (MobiCom)*. 607–622.
- [32] Dong Ma, Guohao Lan, Mahbub Hassan, Wen Hu, Mushfika B Upama, Ashraf Uddin, and Moustafa Youssef. 2019. Solargest: Ubiquitous and battery-free gesture recognition using solar cells. In *The 25th annual international conference on mobile computing and networking*. 1–15.
 - [33] Jingna Mao and Zhiwei Zhang. 2020. Investigation on the Human Body as A Monopole Antenna for Energy Harvesting. In *Proceedings of IEEE EMBC*. 4169–4174.
 - [34] Jingna Mao, Jian Zhao, Huazhong Yang, and et. al. 2017. Using human body as a monopole antenna for energy harvesting from ambient electromagnetic energy. In *Proceedings of IEEE BioCAS*. 1–4.
 - [35] Subhas Chandra Mukhopadhyay. 2014. Wearable sensors for human activity monitoring: A review. *IEEE sensors journal* 15, 3 (2014), 1321–1330.
 - [36] Meinard Müller. 2007. Dynamic time warping. *Information retrieval for music and motion* (2007), 69–84.
 - [37] Kai Niu, Fusang Zhang, Jie Xiong, Xiang Li, Enze Yi, and Daqing Zhang. 2018. Boosting fine-grained activity sensing by embracing wireless multipath effects. In *ACM International Conference on emerging Networking EXperiments and Technologies (CONECT)*. ACM, 139–151.
 - [38] Lawrence R Rabiner. 1978. *Digital processing of speech signals*. Pearson Education India.
 - [39] Yili Ren, Zi Wang, Sheng Tan, Yingying Chen, and Jie Yang. 2021. Winect: 3d human pose tracking for free-form activity using commodity wifi. *ACM on Interactive, Mobile, Wearable and Ubiquitous Technologies (IMWUT)* 5, 4 (2021), 1–29.
 - [40] Anthony Rowe, Vikram Gupta, and Ragunathan Rajkumar. 2009. Low-power clock synchronization using electromagnetic energy radiating from ac power lines. In *Proceedings of the 7th ACM Conference on Embedded Networked Sensor Systems*. 211–224.
 - [41] Alice Ryan and Dariush Elahi. 2007. *Body: Composition, Weight, Height, and Build*. 177–186. <https://doi.org/10.1016/B0-12-370870-2/00024-X>
 - [42] Syed Aziz Shah and Francesco Fioranelli. 2019. RF sensing technologies for assisted daily living in healthcare: A comprehensive review. *IEEE Aerospace and Electronic Systems Magazine* 34, 11 (2019), 26–44.
 - [43] Ruiyuan Song, Dongheng Zhang, Zhi Wu, Cong Yu, Chunyang Xie, Shuai Yang, Yang Hu, and Yan Chen. 2022. Rf-url: unsupervised representation learning for rf sensing. In *Proceedings of the 28th Annual International Conference on Mobile Computing And Networking*. 282–295.
 - [44] Erich P Stuntebeck, Shwetak N Patel, Thomas Robertson, Matthew S Reynolds, and Gregory D Abowd. 2008. Wideband powerline positioning for indoor localization. In *Proceedings of the 10th international conference on Ubiquitous computing*. 94–103.
 - [45] Yonglong Tian, Guang-He Lee, Hao He, Chen-Yu Hsu, and Dina Katabi. 2018. RF-based fall monitoring using convolutional neural networks. *ACM on Interactive, Mobile, Wearable and Ubiquitous Technologies (IMWUT)* 2, 3 (2018), 1–24.
 - [46] Saffet Vatansever and Ahmet Emir Dirik. 2016. Forensic analysis of digital audio recordings based on acoustic mains hum. In *2016 24th Signal Processing and Communication Application Conference (SIU)*. Ieee, 1285–1288.
 - [47] Lochan Verma, Mohammad Fakharzadeh, and Sunghyun Choi. 2013. Wifi on steroids: 802.11 ac and 802.11 ad. *IEEE Wireless Communications* 20, 6 (2013), 30–35.
 - [48] Marinus T Vlaardingerbroek and Jacques A Boer. 2013. *Magnetic resonance imaging: theory and practice*. Springer Science & Business Media.
 - [49] Hao Wang, Daqing Zhang, Yasha Wang, Junyi Ma, Yuxiang Wang, and Shengjie Li. 2016. RT-Fall: A real-time and contactless fall detection system with commodity WiFi devices. *IEEE Transactions on Mobile Computing* 16, 2 (2016), 511–526.
 - [50] Xueyi Wang, Joshua Ellul, and George Azzopardi. 2020. Elderly fall detection systems: A literature survey. *Frontiers in Robotics and AI* 7 (2020), 71.
 - [51] Xuanzhi Wang, Kai Niu, Jie Xiong, Bochong Qian, Zhiyun Yao, Tairong Lou, and Daqing Zhang. 2022. Placement matters: Understanding the effects of device placement for WiFi sensing. *Proceedings of the ACM on Interactive, Mobile, Wearable and Ubiquitous Technologies* 6, 1 (2022), 1–25.
 - [52] Roald K Wangness and Ronald K Wangness. 1979. *Electromagnetic fields*.
 - [53] Leigh C Ward. 2019. Bioelectrical impedance analysis for body composition assessment: reflections on accuracy, clinical utility, and standardisation. *European journal of clinical nutrition* 73, 2 (2019), 194–199.
 - [54] William T Webb and Lajos Hanzo. 1994. *Modern Quadrature Amplitude Modulation: Principles and applications for fixed and wireless channels: one*. IEEE Press-John Wiley.
 - [55] Binbin Xie, Minhao Cui, Deepak Ganesan, Xiangru Chen, and Jie Xiong. 2023. Boosting the Long Range Sensing Potential of LoRa. In *Proceedings of the 21st Annual International Conference on Mobile Systems, Applications and Services*. 177–190.
 - [56] Binbin Xie, Jie Xiong, Xiaojiang Chen, and Dingyi Fang. 2020. Exploring commodity rfid for contactless sub-millimeter vibration sensing. In *ACM Conference on Embedded Networked Sensor Systems (SenSys)*. 15–27.
 - [57] Kun Yang, Xiaolong Zheng, Jie Xiong, Liang Liu, and Huadong Ma. 2022. WiImg: pushing the limit of WiFi sensing with low transmission rates. In *2022 19th Annual IEEE International Conference on Sensing, Communication, and Networking (SECON)*. IEEE, 1–9.
 - [58] Zheng Yang, Yi Zhang, and Qian Zhang. 2022. Rethinking fall detection with Wi-Fi. *IEEE Transactions on Mobile Computing* (2022).
 - [59] Bohan Yu, Yuxiang Wang, Kai Niu, Youwei Zeng, Tao Gu, Leye Wang, Cuntai Guan, and Daqing Zhang. 2021. WiFi-sleep: Sleep stage monitoring using commodity Wi-Fi devices. *IEEE internet of things journal* 8, 18 (2021), 13900–13913.
 - [60] Shichao Yue, Yuzhe Yang, Hao Wang, Hariharan Rahul, and Dina Katabi. 2020. BodyCompass: Monitoring sleep posture with wireless signals. *ACM on Interactive, Mobile, Wearable and Ubiquitous Technologies (IMWUT)* 4, 2 (2020), 1–25.
 - [61] Youwei Zeng, Dan Wu, Jie Xiong, Enze Yi, Ruiyang Gao, and Daqing Zhang. 2019. FarSense: Pushing the range limit of WiFi-based respiration sensing with CSI ratio of two antennas. *Proceedings of the ACM on Interactive, Mobile, Wearable and Ubiquitous Technologies* 3, 3 (2019), 1–26.
 - [62] Fusang Zhang, Zhaoxin Chang, Jie Xiong, Junqi Ma, Jiazhi Ni, Wenbo Zhang, Beihong Jin, and Daqing Zhang. 2023. Embracing Consumer-level UWB-equipped Devices for Fine-grained Wireless Sensing. *ACM on Interactive, Mobile, Wearable and Ubiquitous Technologies (IMWUT)* 6, 4 (2023), 1–27.
 - [63] Fusang Zhang, Kai Niu, Jie Xiong, Beihong Jin, Tao Gu, Yuhang Jiang, and Daqing Zhang. 2019. Towards a diffraction-based sensing approach on human activity recognition. *Proceedings of the ACM on Interactive, Mobile, Wearable and Ubiquitous Technologies* 3, 1 (2019), 1–25.
 - [64] Fusang Zhang, Zhi Wang, Beihong Jin, Jie Xiong, and Daqing Zhang. 2020. Your Smart Speaker Can "Hear" Your Heartbeat! *Proceedings of the ACM on Interactive, Mobile, Wearable and Ubiquitous Technologies* 4, 4 (2020), 1–24.
 - [65] Fusang Zhang, Jie Xiong, Zhaoxin Chang, Junqi Ma, and Daqing Zhang. 2022. Mobi2Sense: empowering wireless sensing with mobility. In *Proceedings of the 28th Annual International Conference on Mobile Computing And Networking*. 268–281.